

# Analytical prediction of sub–surface thermal history in translucent tissue phantoms during plasmonic photo–thermotherapy

Purbarun Dhar<sup>§, #</sup>, Anup Paul<sup>§, ▲</sup>, Arunn Narasimhan and Sarit K Das<sup>\*</sup>

Department of Mechanical Engineering, Indian Institute of Technology, Madras,  
Chennai – 600 036, India

#E–mail: [pdhar1990@gmail.com](mailto:pdhar1990@gmail.com)

▲E–mail: [catchapu@gmail.com](mailto:catchapu@gmail.com)

\*Corresponding author: E-mail: [skdas@iitm.ac.in](mailto:skdas@iitm.ac.in)

§ These authors have contributed equally to this research work.

## Abstract

Knowledge of thermal history in biological tissues during laser based hyperthermia is essential to achieve necrosis of tumour/carcinoma cells. A semi–analytical model to predict sub–surface thermal history in translucent, soft, bio–tissue mimics has been proposed. The model can accurately predict the spatio–temporal temperature variations along depth and the anomalous thermal behaviour in such media, viz. occurrence of sub–surface temperature peaks. Based on opto–thermal properties, the augmented temperature and shift of the peak positions in case of gold nanostructure mediated tissue phantom hyperthermia can be predicted. Employing inverse approach, the absorbance coefficient of nano–graphene infused tissue mimics is determined from the peak temperature and found to provide appreciably accurate predictions along depth. Furthermore, a simplistic, dimensionally consistent correlation to theoretically determine the position of the peak in such media is proposed and found to be consistent with experiments and computations. The model shows promise in predicting thermal history in optically active soft matter and deduction of therapeutic hyperthermia parameters, thereby reducing need for clinical trials.

---

**Keywords:** Laser hyperthermia, tissue mimics, bio heat transfer, gold nanostructures, graphene, PPTT, analytical model

---

## 1. Introduction

Treatment of surface or sub-surface benign tumours or carcinoma cells via hyperthermia induced cellular necrosis (Ritchie et al., 1994), (Simanovskii et al., 2006) and (Lapotko et al., 2006) holds promise as a potential clinical therapy. Among the many techniques of hypothermic therapy, such as magnetic nanoparticle and field assisted hyperthermia (Hilger et al., 2002), (Dombrovsky et al., 2012), (Sturesson and Andersson-Engels, 1995) and (Jeun et al., 2009), ultrasonics assisted hyperthermia (Floch et al., 1999), (Hynynen et al., 1987) and (Diederich and Hynynen, 1999), microwave mediated hyperthermia (Lyons et al., 1984) and (Billard et al., 1990), plasmonic nanostructures assisted photothermotherapy (O'Neal et al., 2004), (Dickerson et al., 2008), (Hirsch et al., 2003) and (Markovic et al., 2011) etc., the last has elicited much attention in recent years due to ease of implementation, possibility of process optimizations and patient compatibility.

Understanding the thermal history within tissues during laser ablation therapy is critical to enable necrosis of diseased cells and ensure safety of healthy neighbouring tissues. However, research has been mostly restricted to *in-vitro* experiments on tissue phantoms (Ghosh et al., 2014), (Paul et al., 2014b), (Jaunich et al., 2008) or *in-vivo* animal trials (von Maltzahn et al., 2009), (O'Neal et al., 2004), (Yang et al., 2010), wherein determining thermal history is often non-feasible. The present letter proposes a simplistic semi-analytical methodology to solve the governing transport equations to determine the spatio-temporal sub-surface thermal history within translucent tissue phantoms during laser ablation. The regions of sub-surface temperature peak and thermal history in gold and graphene nanostructure infused phantoms are deduced based on opto-thermal properties. The predictions are accurate when compared to experiments

and hold promise in theoretical understanding of the process and easy parameter estimation, thereby reducing exhaustive clinical trials.

## **2. Theoretical Formulation**

The experimental methodology and instrumentation were as reported in earlier work (Sahoo et al., 2014) (Ghosh et al., 2014), (Paul et al., 2014b) and a schematic is shown in Fig. 1. Agar gel, prepared in accordance with protocol (Paul et al., 2014b) was utilized as the tissue phantom and a diode-pumped 1064 nm near infrared (owing to maximum absorptivity by bio-tissues) laser was used as the source. Owing to the non-homogeneity associated with soft matter such as tissue phantoms, experiments were repeated five times and the mean value was reported, along with the associated experimental uncertainties. Thermocouples were placed radially with depth-wise spacing of 2.5 mm and hence the error in predictability of position was incorporated.

The process was also computationally simulated in accordance with methodology (Paul et al., 2014a) (Ghosh et al., 2014) using commercial solver Comsol 4.2. The computational domain was taken as a cylindrical section of tissue phantom as shown in Fig. 1 and grid independence was performed (Ghosh et al., 2014).

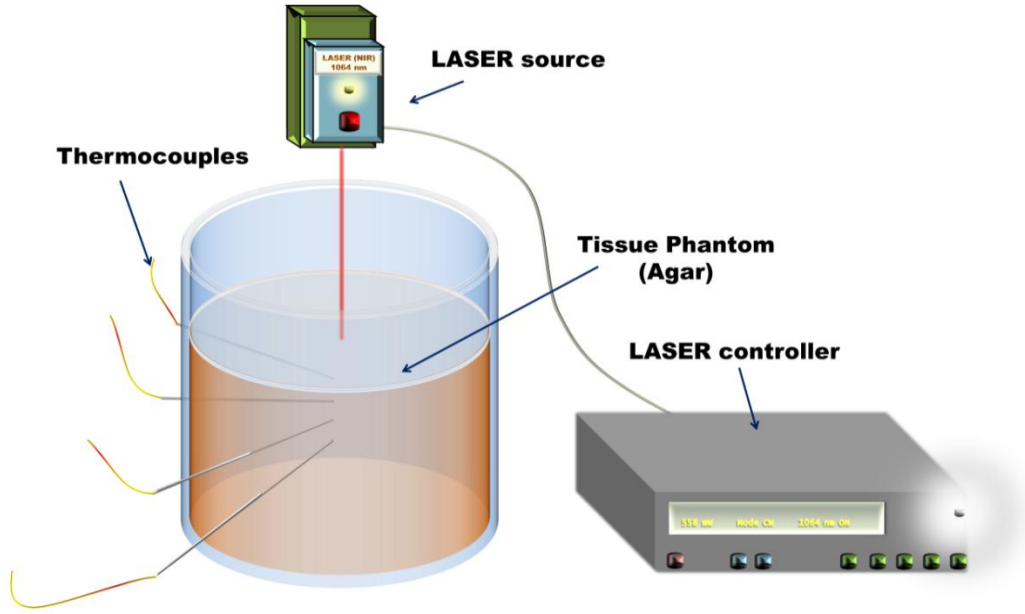


**Figure 1:** The experimental setup. The laser utilized is a diode-pumped solid state 1064 nm near infrared laser. Thermocouples are 1.5 mm J type connected to data acquisition system.

The major governing transport equation for the system exposed to heating by an incident laser beam is

$$k\nabla^2 T + Q_{laser} = \rho C_p \frac{\partial T}{\partial t} \quad (1)$$

where, ' $T$ ', ' $Q_{laser}$ ', ' $k$ ', ' $\rho$ ' and ' $C_p$ ' represent the temperature, laser induced volumetric heat generation, thermal conductivity, density and the specific heat respectively. The heat conduction equation has been solved by disassembling it into a pseudo-steady state system at the termination of thermotherapy process and a transient form tracing the evolution of temperature at various depths of the tissue at a given time frame. Since experiments have been performed on tissue phantoms, the metabolic thermo-generation as well as the micro-perfusion components has not been considered. The objective lies in obtaining a purely steady state and another purely transient governing equation for the phantom so as to arrive at the two extreme possible solutions for the temperature

distribution within the system. The two equations are solved independently to obtain a semi-analytical solution which is further modified utilizing thermophysical properties weighted mean to obtain the thermal history within the tissue phantom during the laser mediated heating process. The spatial form of the equation considering single scattering light–tissue interaction model (Welch, 1984) for the laser induced thermo-generation is expressed in Eqn. (2), wherein the tissue has been considered to attain a steady state at the termination of laser thermotherapy and all transient effects are assumed to be non-existent. Single scattering model has been used in the spatial component of the equation since after achievement of steady state, the thermo-generation due to multiple scattering (Ghosh et al., 2014) plays no further role in enhancement of temperature and the system only transmits absorbed energy within itself, behaving as a single scattering system. Furthermore, this essentially reduces the complexity of the spatial transport equation. The distribution of photonic intensity (of a laser beam with Gaussian energy profile) within the soft material at any spatial location can be expressed in accordance to Beer–Lambert law (Welch, 1984). The governing equation for the spatial component can be expressed as

$$k\nabla^2 T + (\alpha I_0) \exp\left\{\frac{-r^2}{2\sigma^2 \exp(-\beta z)}\right\} \exp\{-(\alpha + \beta)z\} = 0 \quad (2)$$

where, ' $I_0$ ', ' $\alpha$ ', ' $\beta$ ' and ' $\sigma$ ' are the beam intensity, the absorption and scattering coefficients of the tissue phantom and the standard deviation governing the decay of intensity within the translucent medium respectively.

The single and multiple scattering models for light–tissue interactions essentially differ with respect to the nature of photon propagation across the translucent medium (Ghosh et al., 2014). The single scattering model solely considers propagation of

photons along the direction of the beam by forward scattering from the tissue phantom molecules, thereby leading to absorption based heat generation. In contrast, the multiple scattering model encompasses both forward and back scattering by the medium molecules, leading to enhanced interaction of the photons with the phantom molecules, thereby leading to augmented heat generation by both absorption and scattering mechanisms, which is further enhanced due to the presence of plasmonic nanostructures. A representation of the single and multiple scattering effects with and without nanostructures is shown in Fig. 2.

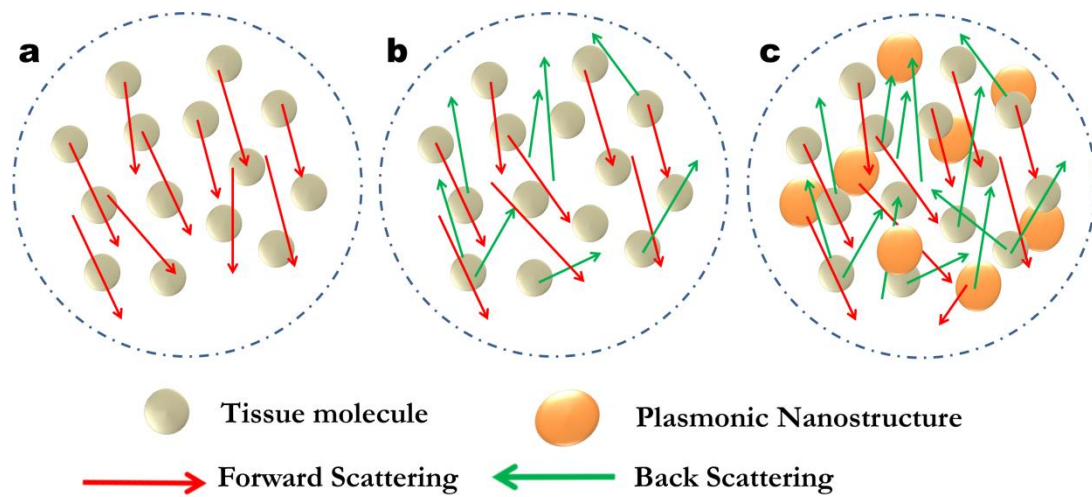


**Figure 2:** Representation of the single scattering light-matter interactions in (a) bare tissue phantom and multiple scattering light-matter interactions in (b) bare phantom and (c) tissue phantom impregnated with plasmonic nanostructures.

The present approach solely encompasses unidirectional thermal effects in the tissue phantom (along depth,  $z$ , considered positive along the direction of laser impingement on the surface) in order to obtain semi-analytical solution for the equation. The radial spatial component  $r$ , comprising the x and y components of location, is thereby reduced

to zero, and assuming isotropic thermal conductivity for the tissue phantom along depth, the equation reduces to its final form as

$$\frac{d^2T}{dz^2} + \left( \frac{\alpha I_0}{k} \right) \exp\{-(\alpha + \beta)z\} = 0 \quad (3)$$

The second order equation is solved based on two boundary conditions that are expected to exist at the time frame wherein the system has been considered to attain a pseudo-steady state, i.e. at termination of thermo-therapy ( $t=t_f$ ). At this instant, a Dirichlet type temperature boundary condition ( $T_{surf, t=t_f}$ ) is imposed on the surface (subscripted as 'surf'), as deduced from thermo-therapy experiments. In cases wherein temperature data at any intermediate time frame during heating is required, that particular time frame is considered as  $t_f$  to obtain that particular solution. Furthermore, the tissue phantom is modelled as a semi-infinite thermo-sink, such that diffusive transport of heat at very high magnitude of depths is considered to be negligible during the event of thermo-therapy. Thus, a Neumann type adiabatic pseudo-boundary condition is imposed to the phantom, such that as the limits of depth tend to infinity and the thermal gradient along depth decays. Based on the above discussion, the solution for Eqn. 3 can be expressed as

$$T_s(z, t = t_f) = T_{surf, t=t_f} + \left[ \frac{\alpha I_0}{k(\alpha + \beta)^2} \right] \{1 - \exp(-(\alpha + \beta)z)\} \quad (4)$$

The solution for the steady component, when evaluated at the time corresponding to termination of thermo-therapy with the surface temperature at that time frame as the sole experimental input, yields the spatial pseudo thermo-history within the tissue phantom at that time instant.

The temporal variance of subsurface temperature within the tissue phantom can be evaluated from the transient analysis of the energy equation (Eqn. 1). It is remodelled

to mimic a system wherein the thermal wave travels only due to temporal laser induced heating and the progressive depth-wise diffusivity along space is considered to be absent. For such a system, the spatial thermal gradients disappear and the transient equation is expressed as

$$\rho C_p \frac{dT}{dt} - (\alpha I_0) \exp\left\{\frac{-r^2}{2\sigma^2 \exp(-\beta z)}\right\} \exp(-\alpha z) \{1 - \exp(-\beta z)\} = 0 \quad (5)$$

The form of Eqn. 5 implies that it can track the thermo-evolution at a point within the tissue and hence the process of thermal transport is not solely governed by absorbance. The tissue, owing to its opto-thermal properties, also participates in the process of scattering the absorbed incident radiation to the surrounding regions and towards the direction of the radiant source itself, leading to a phenomenon termed multiple scattering (Ghosh et al., 2014) (Sahoo et al., 2014), which in turn leads to the formation of sub-surface zone of temperature maxima. The laser induced thermo-generation source term in eqn. 5 has been modelled based on the modified optical parameters for the tissue phantom (DasGupta et al., 2009), to incorporate the multiple scattering effect. Similar to the spatial equation, the component of diffused heat in the radial direction is neglected, leading to the final form (assuming isotropic thermal diffusivity and volumetric heat capacity) of the transient equation as

$$\frac{dT}{dt} - \left(\frac{\alpha I_0}{\rho C_p}\right) \exp(-\alpha z) \{1 - \exp(-\beta z)\} = 0 \quad (6)$$

The equation is solved based on the temperature of the tissue phantom just prior to the inception of the thermo-therapy taken as the initial condition ( $T_i$ ). The solution for thermal evolution at any depth,  $z_c$ , within the tissue phantom for duration of thermo-therapy ( $t$ ) can be expressed as

$$T_T(z = z_c, t) = T_i + \left[ \left(\frac{\alpha I_0}{\rho C_p}\right) \exp(-\alpha z) \{1 - \exp(-\beta z)\} \right] t \quad (7)$$

Equations 4 and 7 provide the temperature along depth for a frozen frame of time and the evolution of temperature with time at a particular depth, respectively. When effectively conglomerated, the two can provide the full thermal history within the phantom, for any depth and for any given duration of heating, provided the initial temperature of the phantom and the surface temperature of the phantom at the frozen instant of time are known. However, since the methodology is semi-analytical in nature, the two solutions cannot be averaged. Instead, a thermophysical properties based weighted average ( $T(z,t)$ ), as expressed in Eqn. 8, has been found to consistently yield accurate predictions.

$$T(z,t) = \frac{T_s(z,t=t_f)Bi + T_T(z=z_c,t)Fo}{Bi + Fo} \quad (8)$$

In Eqn. 8, Bi and Fo represent the Biot and the Fourier numbers associated with the heat transfer process in the tissue phantom respectively. The two non-dimensional parameters are determined based on the characteristic length scale of the phantom (in the present case of a cylindrical domain, the length is one sixth of the cylinder diameter) and the characteristic time, considered as the duration of heating. Predictions obtained from the semi-analytical model for bare tissue phantom for different power levels of the incident beam have been compared against data obtained from full-scale 3D computations and experimental data and are shown in Fig. 3.

### 3. Results and Dsicussions

Thermal history in translucent, soft tissue mimics exhibits counter-intuitive characteristics wherein the peak temperature zone is formed in sub-surface regions rather than at the surface(Ghosh et al., 2014). This occurs due to the multiple-scattering effect

by the tissue material. The present model is observed to accurately predict the phenomenon. However, the predictability of the model is confined to depths just surpassing the region of peak temperature. As the depth increases beyond the peak zone, the model predicts higher values of temperature compared to experiments. Such anomaly can be explained on the basis of the multiple scattering theory and the simplistic nature of the proposed model.

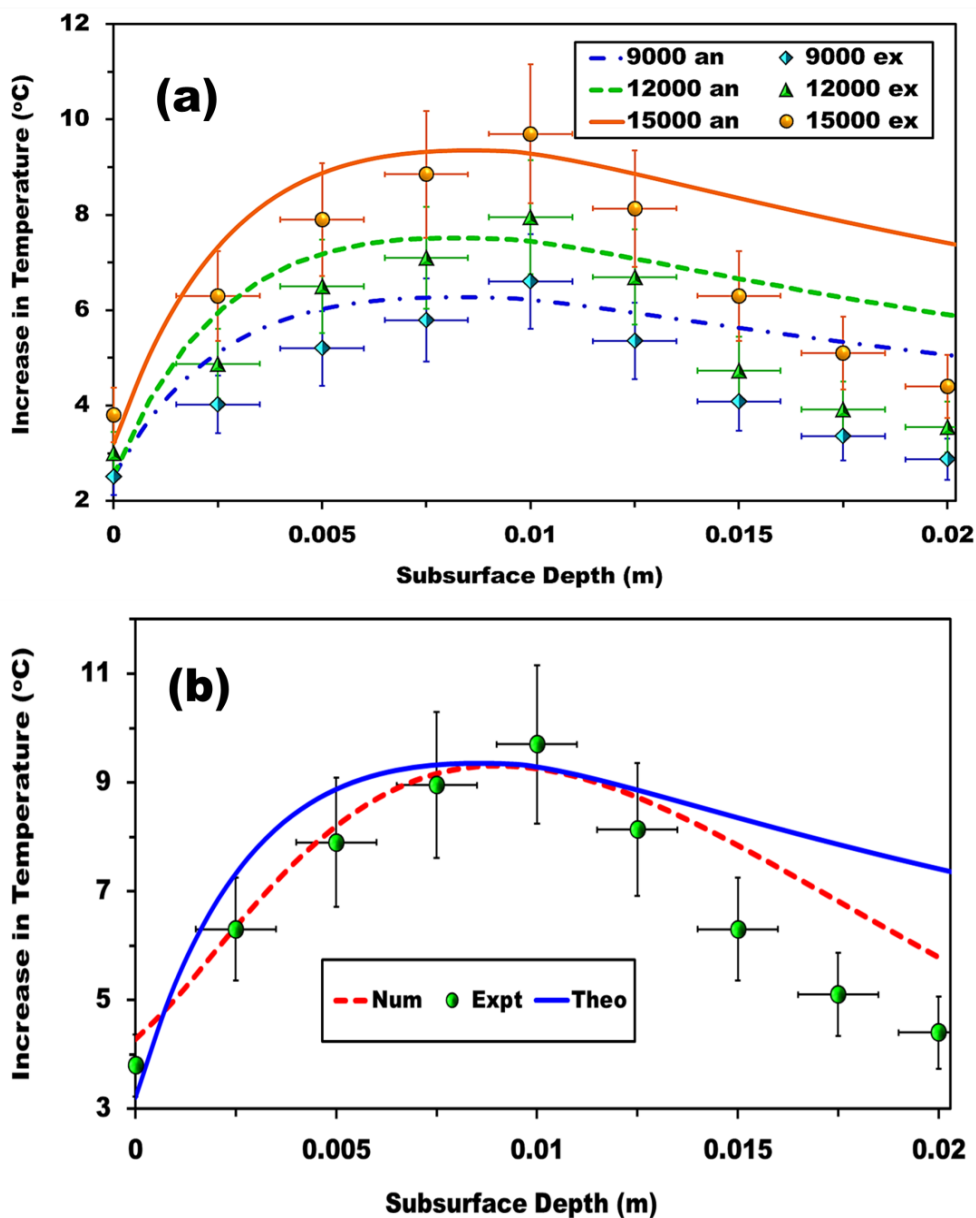


**Figure 3:** (a) Analytical predictions (labelled ‘an’) of sub-surface temperature in bare tissue phantoms for various laser power levels compared against experimental data

(labelled '*ex*') **(b)** Comparative plot for the analytical solution (labelled '*theo*') with respect to complete 3D simulations ('*num*') against experiments ('*expt*').

The occurrence of temperature peak sub-surface occurs due to the interactivities of the forward and the back scattering. As depth increases below surface, the back scattering effect increases due to increased population of medium molecules that the photons encounter, and consequently the temperature rises. However, with depth, the absorbance simultaneously decreases due to intensity attenuation and absorbance in the radial directions and thereby the amount of energy available for scattering reduces. At the peak zone, the two effects converge to reach optima, thereby leading to the formation of a temperature peak. Beyond this region, the available energy decays to limits where scattering cannot predominate and the temperature decreases sharply.

The present model is 1D and, in order to obtain analytical solutions, encompasses neither the beam attenuation nor the absorbance in directions orthogonal to the laser incidence. Consequently, the model cannot track the decay of beam intensity with depth. The intensity thereby remains constant and equivalent to the intensity at the surface. Mathematically, this leads to prediction of enhanced values of temperature in regions wherein the intensity is highly diminished, i.e. at depths beyond the temperature peak, as observed in Fig. 3(a). In the region below the surface and up to the peak zone, the model accurately predicts the thermal history, the accuracy comparable to the predictions from intensive 3D simulations, as shown in Fig. 3(b). Beyond the peak, the sharp decay of temperature is captured by the simulations, however, only qualitatively. Quantitatively, the computational predictions also fail to predict the thermal response accurately, which is further amplified in case of the analytical predictions. However, as far as predictability of the peak temperature and its location and thermal history up to the

peak are concerned, the analytical model shows great potential for accurate mapping of sub-surface thermal history in such media.

During laser aided photo-thermal heat deposition, the penetrability of the photons through the soft matter is a function of the optical response characteristics of the tissue phantom material (DasGupta et al., 2009). Among other optical properties, the absorption and scattering coefficients of the material are of utmost importance for collimated beam based heating. Interestingly, these two properties are tunable and can be tuned to required magnitudes by addition of optically responsive materials; for example, plasmonic nanostructures; to the soft matter. Such nanostructures interact with the bombarding photons and by virtue of surface plasmon response from their surface electron clouds, lead to highly concentrated, localized thermo-generation, which via subsequent absorption and scattering, lead to higher temperatures within the soft matter for the same duration and power of irradiation. Given that the absorbance characteristics ( $\sim 40 \text{ m}^{-1}$ ) of NIR radiation (utilized considering *in-vivo* observations (DasGupta et al., 2009) (Ghosh et al., 2014)) for such tissue mimics is nearly an order of magnitude less compared to its scattering potential ( $\sim 530 \text{ m}^{-1}$ ), addition of nanostructures to augment opto-thermal efficiency is a highly sought methodology in the field of Plasmonic Photo-Thermo-Therapy (PPTT) (Schmidt et al., 2008) (von Maltzahn et al., 2009) (Yang et al., 2010).

The addition of plasmonic nanostructures enhances the absorption characteristics of the tissue mimic, leading to higher heat generation. The present study reports use of two different types of such materials; gold mesoflowers and graphene nanoflakes, both exhibiting very high plasmon response in the NIR window. The absorption coefficient for the particle laden tissue increases to  $\sim 225 \pm 25 \text{ m}^{-1}$  and  $\sim 175 \pm 25 \text{ m}^{-1}$  for gold

mesoflowers (Au) concentrations of 0.3 and 0.2 wt. % respectively (Ghosh et al., 2014). However, the scattering coefficient remains more or less equal to that of bare tissue. The enhanced absorption coefficient leads to higher heat generation within the tissue phantom, leading to higher sub-surface temperatures. Furthermore, the enhanced rise in temperature leads to shift of the peak zone towards the surface. The predictability of the model for Au laden tissue mimics against experimental observations and the comparative with computations have been illustrated in Fig. 4(a) and 4(b) respectively.

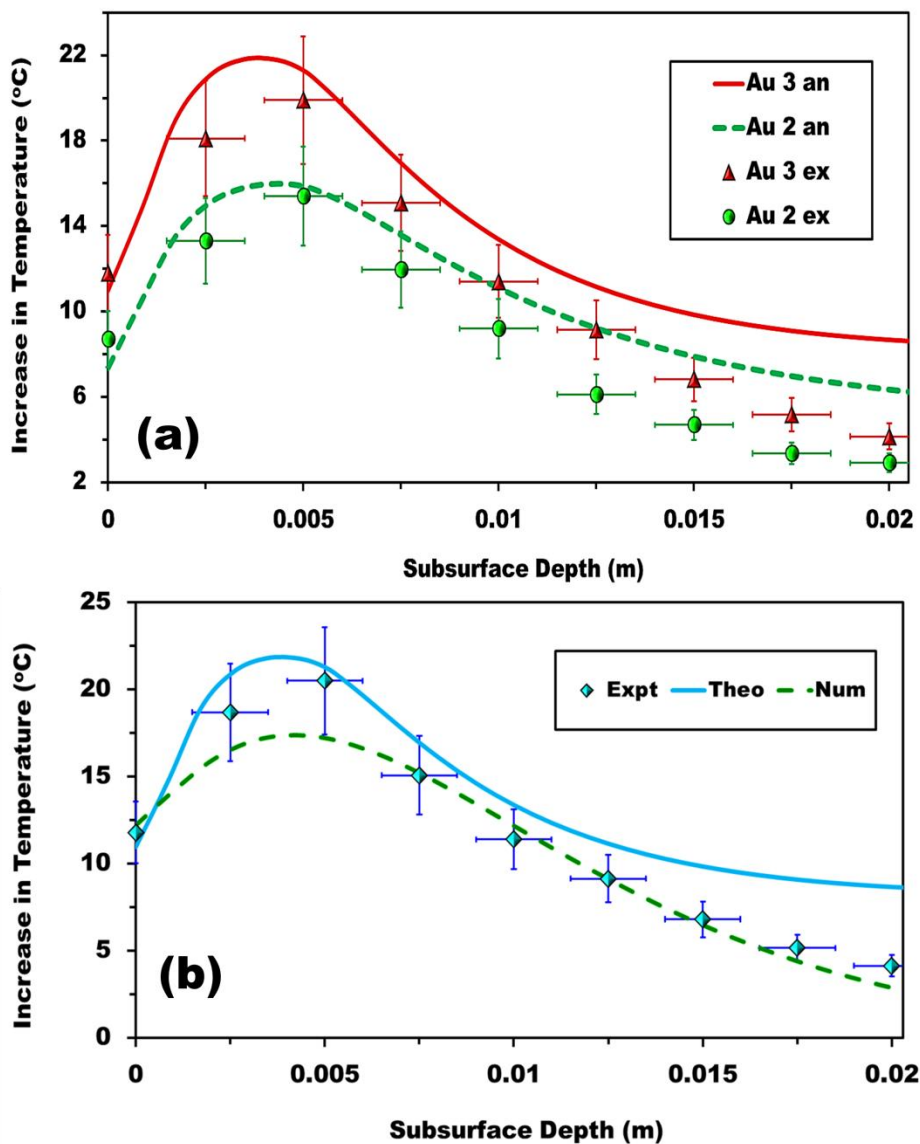


**Figure 4:** (a) Analytical predictions (labelled '*an*') of sub-surface temperature in Au mesoflowers infused bare tissue phantoms for various concentrations (3 mg and 2 mg per gram phantom) compared against experimental data (labelled '*ex*') (b) Comparative plot for the analytical solution (labelled '*theo*') with respect to simulations ('*num*') against experiments ('*expl*').

The present study also includes a dimensionally consistent, intuitive correlation to determine the depth at which peak temperature is expected to manifest upon exposure to surface heating, given that ' $\alpha$ ' and ' $\beta$ ' for the translucent soft matter is known. It is possible to deduce the peak depth ( $z_p$ ) theoretically for such substances; the correlation being expressed as

$$z_p \approx \sqrt{\frac{2}{\alpha\beta}} \quad (9)$$

The theoretical predictions for peak depth for bare and Au infused tissue phantoms have been compared against experimental and computational results in Fig. 5 and have been found to be accurate.

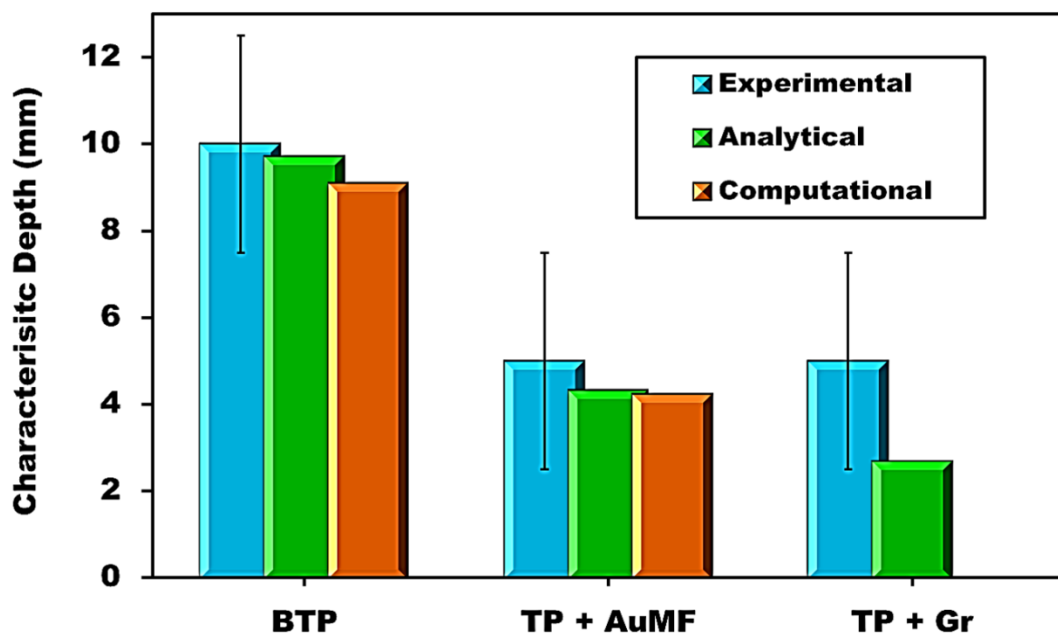


**Figure 5:** Analytical predictions position of sub-surface temperature peak against computational results and experimental data. TP, B, MF and Gr refer to tissue phantom, bare, mesoflowers and graphene respectively. The model also accurately predicts the findings reported (Ghosh et al., 2014) in literature.

Opto-thermal properties of tissue phantoms embedded with graphene nanoflakes are non-existent in literature and an inverse methodology has been adopted to determine the same. As observed from Figures 3(a) and 4(a), the present model can predict the temperatures below surface up to the peak temperature with good accuracy. Furthermore, as expressed in Eqn. 9, it is possible to determine the peak zone from opto-thermal properties. Assuming that similar to Au laden tissues ' $\beta$ ' remains unaffected, from Eqn. 9, it is possible to express ' $\alpha$ ' in terms of ' $z$ '. Utilizing the expression for ' $z$ ' in Eqns. 4 and 7, and obtaining two equations from Eqn. 8 for the experimental peak and immediate neighbouring point temperatures, it is possible to deduce ' $\alpha$ ' for tissue phantoms infused with graphene nanoflakes and the present analysis yields a value of  $\sim 600 \text{ m}^{-1}$  for the same. Based on the obtained value, the peak depth is determined from Eqn. (9) and compared against experiments in Fig. 5. Similarly, the complete sub-surface thermal history is predicted and compared against experiments in Fig. 6, wherein good accuracy is observed. This essentially establishes that the obtained value of ' $\alpha$ ' for graphene infused phantoms is accurate. However, the enhanced absorptivity should lead to shift of the peak zone towards surface as compared to Au. This is not observed in experiments, which may be attributed to the spacing of the thermocouples. The predicted peak position however lies within the ranges of positional uncertainty (Fig. 6) and thereby the experimental deviations are justified.

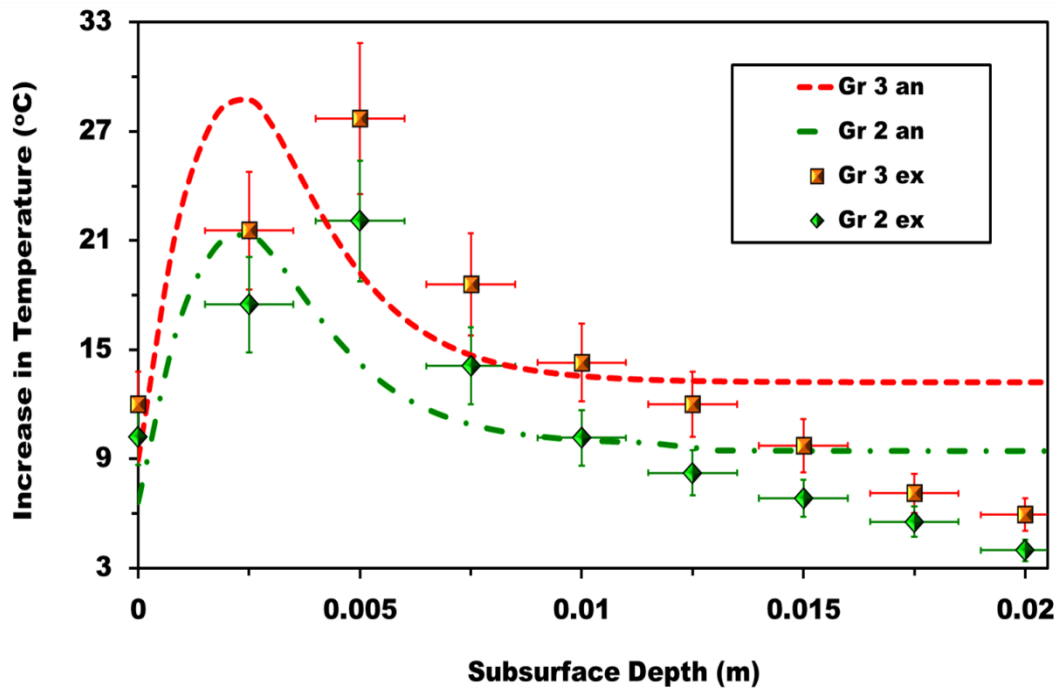


**Figure 6:** Analytical predictions (labelled ‘an’) of sub-surface temperature in Graphene infused bare tissue phantoms for various concentrations (3 mg and 2 mg per gram phantom) compared against experimental data (labelled ‘ex’).

#### 4. Conclusion

To conclude, a semi-analytical mathematical model so to predict the sub-surface thermal history in translucent, soft, bio-tissue mimics has been proposed. The present model is capable of deducing the spatio-temporal variations in temperatures along depth and can also accurately predict the anomalous thermal behaviour in such media, such as formation of sub-surface thermal peaks. Based on known opto-thermal parameters, the model is capable of predicting augmented temperature and shift of the peak positions in case of gold nanostructure mediated tissue phantom hyperthermia. Based on inverse approach, the absorbance coefficient of graphene infused tissue mimics is determined from the peak temperature and found to provide appreciably accurate predictions throughout the depth range. Furthermore, a simplistic yet dimensionally consistent

correlation to theoretically determine the position of the peak in such media is proposed and found to be consistent with experimental data. The present approach can show potential in the prediction of thermal history in optically active soft matter and deduction of biological hyperthermia parameters. Such predictions can reduce the need for extensive and detailed computations, experimentations and clinical trials.

## Acknowledgements

The authors thank Dr. Shamit Bakshi of the Department of Mechanical Engineering, Indian Institute of Technology Madras, for the NIR laser. PD and AP also thank the Ministry of Human Resource and Development, Govt. of India, for the doctoral research scholarship.

## References

- Billard, B.E., Hynynen, K., Roemer, R.B., 1990. Effects of physical parameters on high temperature ultrasound hyperthermia. *Ultrasound in Medicine & Biology* 16, 409-420.
- DasGupta, D., von Maltzahn, G., Ghosh, S., Bhatia, S.N., Das, S.K., Chakraborty, S., 2009. Probing nanoantenna-directed photothermal destruction of tumors using noninvasive laser irradiation. *Applied Physics Letters* 95, 233701.
- Dickerson, E., Dreaden, E., Huang, X., El-Sayed, I.H., Chu, H., Pushpanketh, S., McDonald, J., El-Sayed, M., 2008. Gold nanorod assisted near-infrared plasmonic photothermal therapy (phtt) of squamous cell carcinoma in mice. *Cancer Letters* 269, 57 – 66.
- Diederich, C.J., Hynynen, K., 1999. Ultrasound technology for hyperthermia. *Ultrasound in Medicine & Biology* 25, 871-887.
- Dombrovsky, L.A., Timchenko, V., Jackson, M., 2012. Indirect heating strategy for laser induced hyperthermia: An advanced thermal model. *International Journal of Heat and Mass Transfer* 55(17-18), 4688-4700.
- Floch, C.L., Tanter, M., Fink, M., 1999. Self-defocusing in ultrasonic hyperthermia: Experiment and simulation. *Applied Physics Letters* 74, 3062-3064.
- Ghosh, S., Sahoo, N., Sajanlal, P., Sarangi, N., Ramesh, N., Panda, T., Pradeep, T., Das, S.K., 2014. Anomalous Subsurface Thermal Behavior in Tissue Mimics Upon Near Infrared Irradiation Mediated Photothermal Therapy. *Journal of Biomedical Nanotechnology* 10, 405-414.
- Hilger, I., Hiergeist, R., Hergt, R., Winnefeld, K., Schubert, H., Kaiser, W., 2002. *Investigative Radiology* 37, 580-586.

- Hirsch, L.R., Stafford, R.J., Bankson, J.A., Sershen, S.R., Rivera, B., Price, R.E., Hazle, J.D., Halas, N.J., West, J.L., 2003. Nanoshell-mediated near-infrared thermal therapy of tumors under magnetic resonance guidance. *Proceedings of the National Academy of Sciences* 100(23), 13549–13554.
- Hynynen, K., Roemer, R., Anhalt, D., Johnson, C., Xu, Z.X., Swindell, W., Cetas, T., 1987. A scanned, focused, multiple transducer ultrasonic system for localized hyperthermia treatments. *International Journal of Hyperthermia* 3, 21-35.
- Jaunich, M., Raje, S., Kim, K., Mitra, K., Guo, Z., 2008. Bio-heat transfer analysis during short pulse laser irradiation of tissues. *International Journal of Heat and Mass Transfer* 51(23-24), 5511–5521.
- Jeun, M., Bae, S., Tomitaka, A., Takemura, Y., Park, K.H., Paek, S.H., Chung, K.-W., 2009. Effects of particle dipole interaction on the ac magnetically induced heating characteristics of ferrite nanoparticles for hyperthermia. *Applied Physics Letters* 95, 082501.
- Lapotko, D., Lukianova, E., Potapnev, M., Aleinikova, O., Oraevsky, A., 2006. Method of laser activated nano-thermolysis for elimination of tumor cells. *Cancer Letters* 239(1), 36-45.
- Lyons, B.E., Britt, R.H., Strohbehn, J., 1984. Localized hyperthermia in the treatment of malignant brain tumors using an interstitial microwave antenna array. *Biomedical Engineering, IEEE Transactions on*, 53-62.
- Markovic, Z.M., Harhaji-Trajkovic, L.M., Todorovic-Markovic, B.M., Kepić, D.P., Arskin, K.M., Jovanović, S.P., Pantovic, A.C., Dramićanin, M.D., Trajkovic, V.S., 2011. In vitro comparison of the photothermal anticancer activity of graphene nanoparticles and carbon nanotubes. *Biomaterials* 32, 1121-1129.
- O’Neal, D., Hirsch, L., Halas, N., Payne, J., West, J., 2004. Photo-thermal tumor ablation in mice using near infrared-absorbing nanoparticles. *Cancer Letters* 209(2), 171 - 176.
- Paul, A., Bandaru, N., Narasimhan, A., Das, S., 2014a. Subsurface Tumor Ablation with Near-infrared Radiation using Intratumoral and Intravenous Injection of Nanoparticles. *International Journal of Micro-Nano Scale Transport* 5, 69-80.
- Paul, A., Narasimhan, A., Kahlen, F., Das, S., 2014b. Temperature evolution in tissues embedded with large blood vessels during photo-thermal heating. *Journal of Thermal Biology* 41, 77-87.
- Ritchie, K.P., Keller, B.M., Syed, K.M., Lepock, J.R., 1994. Hyperthermia (heat shock)-induced protein denaturation in liver, muscle and lens tissue as determined by differential scanning calorimetry. *International Journal of Hyperthermia* 10(5), 605-618.
- Sahoo, N., Ghosh, S., Narasimhan, A., Das, S., 2014. Investigation of non-Fourier effects in bio-tissues during laser assisted photothermal therapy. *International Journal of Thermal Sciences* 76, 208-220.
- Schmidt, A., Alper, J., Chiesa, M., Chen, G., Das, S., Hamad-Schifferli, K., 2008. Probing the Gold Nanorod– Ligand– Solvent Interface by Plasmonic Absorption and Thermal Decay. *Journal of Physical Chemistry C* 112 (35), 13320–13323.
- Simanovskii, D.M., M. A. Mackanos, A. R. Irani, C. E. O’Connell-Rodwell, C. H. Contag, H. A. Schwettman, Palanker, D.V., 2006. Cellular tolerance to pulsed hyperthermia. *Physical Review E* 74, 011915.
- Stureson, C., Andersson-Engels, S., 1995. A mathematical model for predicting the temperature distribution in laser-induced hyperthermia. *experimental*

evaluation and applications. . *Physics in Medicine and Biology* 40(12), 2037–2052.

- von Maltzahn, G., Park, J., Agrawal, A., Bandaru, N., Das, S., Sailor, M., Bhatia, S., 2009. Computationally guided photothermal tumor therapy using long-circulating gold nanorod antennas. *Cancer Research* 69, 3892-3900.
- Welch, A., 1984. The thermal response of laser irradiated tissue. *IEEE Journal of Quantum Electronics* 20(12), 1471–1481.
- Yang, K., Zhang, S., Zhang, G., Sun, X., Lee, S.-T., Liu, Z., 2010. Graphene in mice: ultrahigh in vivo tumor uptake and efficient photothermal therapy. *Nano letters* 10, 3318-3323.